

MULTIPACTING STUDY IN INFN-LASA ESS MEDIUM-BETA CAVITY

J.F. Chen[†], M. Bertucci, A. Bosotti, P. Michelato, L. Monaco, C. Pagani¹, R. Paparella, S. Pirani², D. Sertore, INFN–LASA, Segrate (MI), Italy
¹also at University of Milano, Milan, Italy
²ESS, Lund, Sweden, on leave at INFN-LASA, Segrate (MI), Italy

Abstract

We present Multipacting studies in ESS Medium-Beta cavities of INFN-LASA design with both simulation and experimental results. The simulation on the ideal cavity shape with both FishPact and MultiPac2.1 codes shows that Multipacting appears in a very small region near equator where the weld seam exists. A simulation with more realistic cavity shape considering the weld seam at cell equators has also been done showing similar results for end cell but a remarkable mitigation for inner cell. During the vertical tests at LASA, Multipacting is frequently observed but with no limitation to the cavity performance, which well confirms the MP predicted by the simulations.

INTRODUCTION

The ESS medium-beta cavity prototypes have been designed by INFN-LASA, fabricated at E.Zanon and been cold tested in LASA [1, 2]. During their cold tests, Multipacting (MP) has been observed in both Fine-Grain (FG) and Large-Grain (LG) cavities. For the FG cavity, MP showed only a Q_0 -drop with no impact to the excellent cavity performance. But for the LG cavity, during the first vertical test, the quench field level is exactly at MP region, accompanied with strong X-radiation. Therefore, it is important to investigate the behaviour and effect of MP in these cavities.

The necessary conditions for two-point MP are stable trajectories and Secondary Emission Yields (SEY), $\delta > 1$. The SEY depends on final impacting kinetic energy (E_f) and surface condition. A high SEY curve in Niobium cavity shows the first crossover at an impact energy that can be lower than 30 eV [3]. The actual properties will depend on the cleanliness and chemical treatment of the surface [4]. Figure 1 shows the generic dependence of SEY on the impact energy.

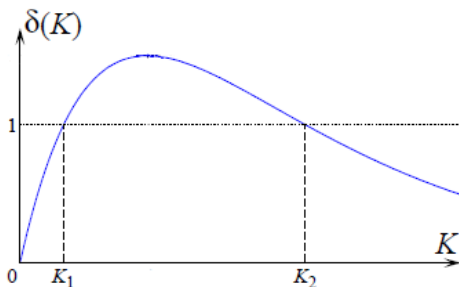


Figure 1: Generic dependence of the SEY on the impact kinetic energy.

The INFN-LASA ESS-MB cavity is designed with spherical equators at both the inner cells and the end cells:

[†] Email address: jinfang.chen@mi.infn.it

in the latter the diameter slightly larger to achieve an uniform field profile [5]. Hence, the MP simulation is taken in these two different type of cells. We have used FishPact [6] for the main simulations, and MultiPac2.1 [7] for cross check.

SIMULATION RESULTS

Firstly, we studied the MP on the ideal cavity design, namely cells with round equator. We find that the two-point MP occurs in a very short distance where the weld seam (width ≥ 4 mm) exists in cell equator. Therefore, a further simulation is also done considering the welding seam, generally a bump on the linear part due to the weld under-bead.

Ideal Shape with Round Equator

The designed cavity shape at 2 K temperature is used. Simulation conditions in FishPact: E_{acc} scanned every 1 MV/m from 1 to 25 MV/m, phase scanned every 10° from 0 to 360° , initial and secondary emission energy set as 2 eV, and emission angle normal to surface.

In theoretical treatments, the E_f is proportional to the emission energy, usually a few eV. This means that an increasing of the emission energy leads to the same increase of the impact energy of the electrons [8, 9]. The default initial and secondary emission energy at 2 eV are adopted in all the simulations in this paper. Concerning the impact angle, studies show a larger enhancement of the SEY for small angles at higher energy, but a small enhancement of SEY at lower energy [10]. Due to the low impact energy in elliptical cavities, we don't expect any SEY dependence on the impact angle.

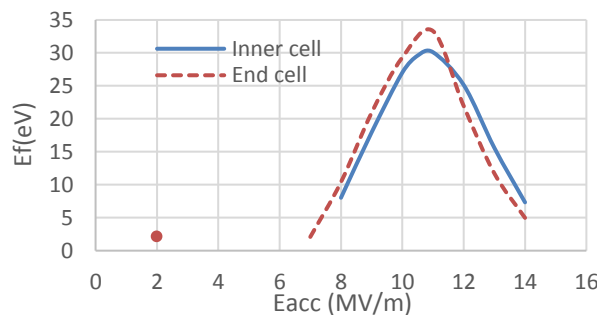


Figure 2: Final impact energy after 20 impacts in inner cell and end cell with round equator (red dot indicates 2nd order two-point MP in end cell).

In INFN-LASA MB cavity design, the 1st order two-point MP occurs in the E_{acc} range from 7 MV/m to 14 MV/m, with maximum E_f of 30 eV and 33 eV at E_{acc} around 11 MV/m for inner cell and end cell, respectively,

as shown in Fig. 2. Since the final impact energy is always less than 40 eV, we do not expect any hard barriers. We do expect only soft barriers if the initial SEY is high enough [3].

Besides, in end cell a 2nd order two-point MP is found at $E_{acc} = 2$ MV/m, with $E_f = 2$ eV as shown in Fig. 2. Due to the small E_f , we don't expect any dangerousness. Nevertheless, it is also observed in the 1st vertical test of the LG cavity.

MultiPac2.1 Cross Check

In order to confirm the above simulation results, we used another widely employed code, MultiPac2.1 for cross-checking the previously obtained results, and consistent results are obtained.

The MP is found in a small region near equator (<1 mm, see Fig. 3). For inner cell, the two impact sites of the MP are symmetric to the equator centre. While for the end cell, the two sites are asymmetric to the equator centre, both on the penultimate half-cell (inside one) due to the asymmetric geometry and field distribution in the end cell.

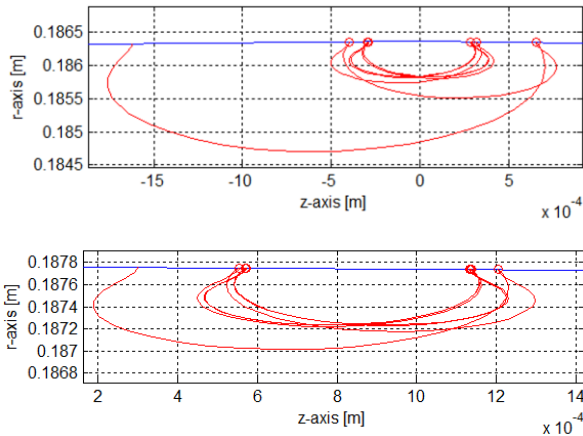


Figure 3: Multipacting trajectories in ideal cells as calculated by MultiPac2.1 for $E_{peak} 29$ MV/m, corresponding to $E_{acc} 11$ MV/m (upper plot: inner cell; lower plot: penultimate half-cell side of the end cell; blue lines are cell profiles).

Equator with Weld Seam

As shown above, the stable MP trajectories occur in a very small region near equator centre where the electron-beam welding takes place during cavity fabrication. The ESS MB cavity prototype is fabricated at the company E.Zanon with a similar preparation as for hundreds of 1.3 GHz TESLA cavities successfully produced for E-XFEL project, including the same electron-beam (EB) welding technology. Due to this similarity, a typical replica of inner equator region from TESLA cavity is used to study the geometry near the equator centre (see Fig. 4, left).

As shown, a typical shape of inner equator after EB welding is a bump about 4 mm width and 0.3 mm height in the equator centre, with a 2 mm linear part at each side connecting it to the round part of cell. This linear under-cut is prepared before EB welding to ensure its full penetration. During welding, the under-bead is formed due to gravity

and shrinkage effects. Based on the replica shape, the equator region is rebuilt for MP simulation by a simple model shown in Fig. 4, right (inner side of the cavity is at the bottom).

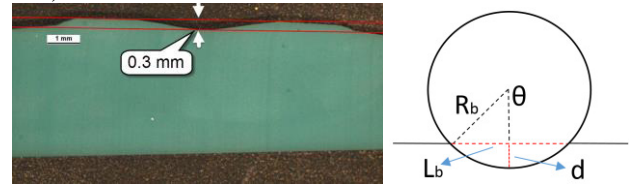


Figure 4: (left) A typical replica of inner equator from TESLA cavity EB-welded at E. Zanon (green part indicates cavity inner side); (right) modeling the bump shape near equator for simulation ($L_b = 4$ mm, $d = 0.3$ mm).

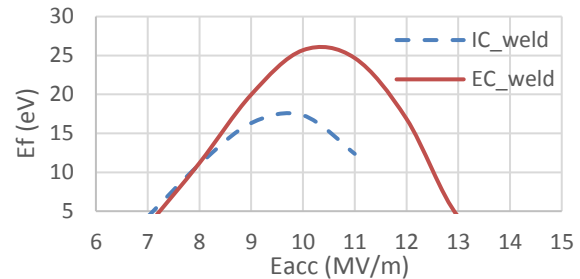


Figure 5: Final impact energy for the cavity considered the weld seam in the cell equators.

With this modified cells shape, a new MP simulation is done using Fishpack. The final impact energy after 20 impacts on both inner cell and end cell is shown in Fig. 5. Interesting to note that the E_f in the inner cell is decreased remarkably with respect to the ideal shape and MP disappears after 11 MV/m, however, E_f in end cell is less reduced, remaining higher than 25 eV. Two MP trajectories at $E_{acc} 11$ MV/m in the inner cell and end cell with weld seam are shown in Fig. 6. The stable trajectories in inner cell are concentrated on the crest of seam, while in end cell they are concentrated on one slope of the bump, again due to the asymmetry of this cell.

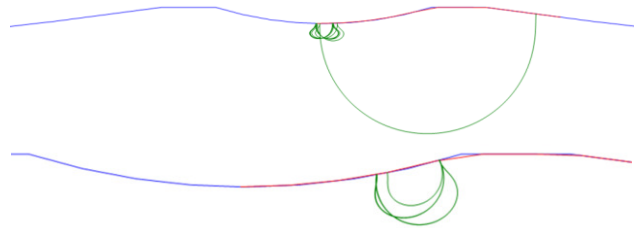


Figure 6: MP trajectories at $E_{acc} 11$ MV/m in the inner cell and in the end cell with weld seam (upper: inner cell; lower: end cell; not in same scale).

EXPERIMENTAL RESULTS

Fine Grain Cavity

MP is observed in the first power rise in which MP starts at $E_{acc} 9$ MV/m. The Q_0 -drop at $E_{acc} = 10$ and 11 MV/m is clearly seen in the Q_0 - E_{acc} curve (shown in Fig. 7), corre-

sponding to the maximum E_f of 1st order two-point MP predicted by the above simulations. Also the field emission recorded during the MP processing is consistent with the simulation.

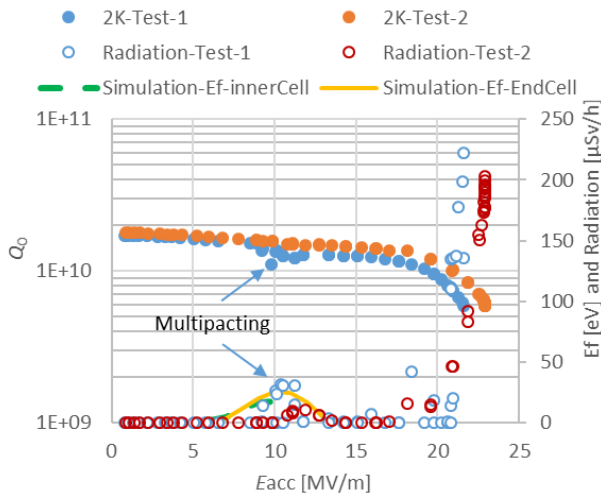


Figure 7: Fine-Grain-cavity vertical test results in INFN-LASA.

During this first power rise, the signal from the 11 Cernox sensors that are mounted on the six equators shows, on the coupler-side end cell, a sharp peak of temperature in the middle of power filling, corresponding to E_{acc} around 11 MV/m (see Fig. 8). This temperature behaviour is recorded together with the envelope of the transmitted power, where the apparent periodicity is given by the cavity power filling and the sharp discharge during quench once the maximum field is reached. Although we have only a few temperature sensors, the fact that only one on the end cell responds when MP happens, suggests that the MP in the end cell is dominant, as shown in Fig. 5. Since the MP occurs on the weld seam, E_f in inner cell is reduced to less than 18 eV when SEY is probably below unity. Figure 8 also shows that a clear decreases of MP-induced temperature after first power filling, corresponding to the RF processing of the MP sites.

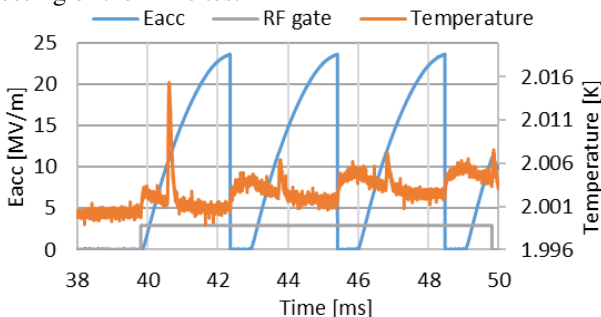


Figure 8: Temperature measurement on the equator of coupler-side end cell during periodic power.

In the second power rise, the Q_0 -drop disappeared. This is probably because the impact energy is very close to the first crossover of the SEY curve, which shifts up after the surface is “cleaned up” by RF processing during measurements [8].

Large Grain Cavity

During the first vertical test of LG cavity, the resonator quenched at $E_{acc} = 10$ MV/m, accompanied with strong Field Emission (FE), which is exactly at the MP field region. Is it dominantly caused by MP? Further tests show negative answer.

In order to study the FE sites, the cavity has also been tested in all the other five passband modes and, in all of them, quenched at almost equal field level, except in $4\pi/6$ mode where E_{acc} reached 13 MV/m. In this mode, we saw a clear Q_0 -drop and strong FE at 10 MV/m, but after only a very short time processing the MP barrier was passed and finally the cavity quenched at higher field level with low FE as shown in Fig. 9. Therefore, we believe that the MP is not limiting the cavity performance but it may give only a subsidiary contribution to the quench. This conclusion has been confirmed in the 2nd test after the cavity has been done a flash BCP and a 24-hours HPR. In this new test, no FE was measured but cavity quenched at the same field level [11, 12].

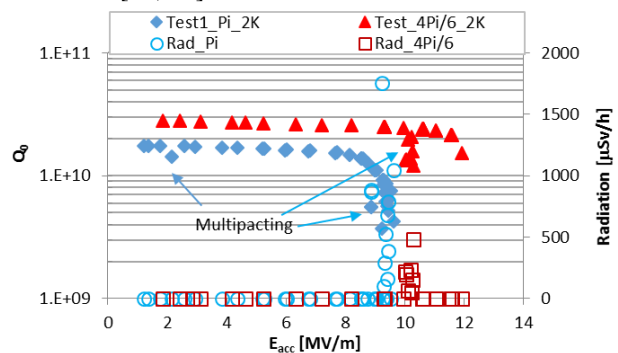


Figure 9: Large-grain-cavity vertical test results in INFN-LASA.

CONCLUSIONS

We have studied the MP phenomenon in ESS-MB cavity of INFN-LASA design with both simulations and experimental results. The simulations have been done on both the ideal cavity shape and the more realistic shape with a weld seam, based on a replica technique. Simulation results show the 1st order 2-point MP appears around E_{acc} 11 MV/m with maximum E_f about 30 eV. Furthermore, it also shows that an under-bead at weld seam can mitigate significantly MP by reducing nearly half of E_f in the symmetric inner cell but only slight decrease in the asymmetric end cell. During the vertical tests at LASA, MP has also been frequently observed in terms of Q_0 -drop and radiation. The simulation and test results are well consistent. Due to the low E_f , MP in ESS MB cavity is considered only a soft barrier and not a limitation to the cavity performance.

REFERENCES

[1] L. Monaco *et al.*, "Fabrication And Treatment Of The Ess Medium Beta Proto-type Cavities ", in *Proc. IPAC'17*, Copenhagen, Denmark, May 2017, this conference.

- [2] A. Bosotti *et al.*, "Vertical tests of ESS Medium Beta Prototype cavities at LASA", in *Proc. IPAC'17*, Copenhagen, Denmark, May 2017, this conference.
- [3] W. Hartung *et al.*, "Studies of Multipacting in Axisymmetric Cavities for medium-velocity beams", in *Proc. SRF'01*, Tsukuba, Japan, 2001, pp.627-631.
- [4] F. L. Krawczyk, "Status of multipacting simulation capabilities for SCRF applications", in *Proc. SRF'01*, Tsukuba, Japan, 2001, pp. 108-114.
- [5] P. Michelato *et al.*, "ESS Medium and High Beta Cavity Prototypes", in *Proc. IPAC'16*, Busan, Korea, May 8-13, 2016, pp. 2138-2140.
- [6] G. Wu *et al.*, "Multipacting analysis for JLab Ampere class cavities", in *Proc. SRF'05*, New York, USA, 2005, pp. 300-302.
- [7] P. Ylä-Oijala and D. Proch, "MultiPac–Multipacting simulation package with 2D FEM field solver", in *Proc. SRF'01*, Tsukuba, Japan, 2001, pp. 105-107.
- [8] R. Geng, "Multipacting simulations for superconducting cavities and RF coupler waveguides", in *Proc. PAC'03*, Portland, USA, 2003, pp. 264-268.
- [9] V. Shemelin, "Multipactor in crossed rf fields on the cavity equator", *Phys. Rev. Accel. Beams*, vol. 16, p. 012002, Jan. 2013.
- [10] B. Henrist *et al.*, "Secondary electron emission data for the simulation of electron cloud", in *Proc. ELOUD'02*, Geneva, Switzerland, 2002.
- [11] D. Sertore *et al.*, "Experience on design, fabrication and testing of a large grain ess medium beta prototype cavity ", in *Proc. IPAC'17*, Copenhagen, Denmark, May 2017, this conference.
- [12] M. Bertucci *et al.*, "Quench and Field Emission Diagnostics for the ESS Medium-Beta Prototypes Vertical Tests at LASA ", in *Proc. IPAC'17*, Copenhagen, Denmark, May 2017, this conference.